Simulated evolutionary optimization of an ion-exchange chromatography step

Fredrik Nielsen

Department of Chemical engineering, Faculty of Engineering, Lund University, Getingevägen 60, 22241, Lund, Sweden

Abstract

This work proposes an optimization scheme for a model-based approach capable of predicting the optimal point of operation regarding productivity for an ion-exchange column. It is based on an evolutionary refinement of model calibration and intermediate optimal operation points. The work aims at minimizing required amount of experimental data for finding the optimal operation point. The chromatographic column is simulated with the equilibrium-dispersive model and a Langmuir isotherm fitted with mobile phase and saturation capacity modulators. The model parameters are initially fitted to few experiments with variable load and gradient slope. Calibration and optimization is performed in an iterative fashion. Each generated optima is run experimentally and added to the experimental data pool to expand the calibration reference material. The iterative process is continued until an adequate fit is obtained. The iterative model calibration and optimization scheme is able to present an adequate fit between experimental and simulated chromatograms, while keeping the amount of experiments at bay. The close elution of the sample proteins and model behavior however leaves room for speculation about the accuracy of individual protein concentration profiles in the column effluent.

Key words: protein; purification; ion-exchange; chromatography; downstream processing; simulation; parameter estimation; optimization

1 Introduction

New applications for biological entities, e.g. proteins, are revealed on regular basis, but the production is still associated with considerable costs. Downstream processing incur up to 80% of total production cost associated with production of proteins. The trend in down stream processing goes towards elimination of purification steps. The reason for this is that approximately 5-30 % of the product is lost in each processing step. Decreasing recovery amasses to tremendous costs, especially when dealing with high value products. In eliminating steps a far greater recovery can be obtained. A prerequisite for being able to reduce the number of process steps is that prevailing process steps can be optimized in a fashion that enables adequate consistency and performance. The primary objective for process scale purification is to minimize cost for a purified product which meets specifications. Computational prediction of optimal operating conditions is one way of significantly reduce costs, labour and amount of experiments required.

This work proposes an optimization scheme for a model-based approach that is capable of predicting the optimal point of operation regarding productivity for an ion-exchange chromatography (IEC) column, while the amount of experiments are kept at a minimum. It is based on an evolutionary refinement of model calibration and optimal operation point.

2 Theory

In liquid chromatography is the feedstock transported in a liquid mobile phase. The mobile phase is forced through an immiscible packed bed, the stationary phase, where it is retained. Mathematical models describing the process are based on differential mass balances over the stationary and mobile phases. This results in a set of differential equations describing protein concentration in space and time.

2.1 Column model

The dispersion and convection within the column can be described with the equilibrium-dispersive model.

$$\frac{\partial c_i}{\partial t} = D_{ax} \cdot \frac{\partial^2 c_i}{\partial x^2} - \upsilon_{\text{int}} \cdot \frac{\partial c_i}{\partial x} - \frac{(1-\varepsilon_c)}{\varepsilon_c} \cdot \frac{\partial q_i}{\partial t} \qquad (1)$$

The equilibrium-dispersive model assumes that all contributions due to non-equilibrium are lumped into the apparent axial dispersion coefficient, D_{ax}. The column must be assumed to be radially homogeneous. Mass transfer in the column must be assumed to be controlled only by molecular diffusion across the mobile phase flowing around the particles and the mass transfer between mobile and stationary phase is fast. The compressibility of the mobile phase is assumed to be negligible and thus can the interstitial velocity be considered constant along the column. The axial dispersion coefficient is assumed to be constant. [1]

The column model is subjected to a Robin boundary condition at the inlet, eqn 2, and a Neumann boundary condition at the column outlet, eqn 3.

$$\frac{\partial c_i}{\partial x} = \frac{\upsilon_{\text{int}}}{D_{ax}} \cdot \left(c_i - c_{inlet,i} \right) \quad \text{at x=0} \tag{2}$$

$$\frac{\partial c_i}{\partial x} = 0 \quad \text{at x=L} \tag{3}$$

2.2 Adsorption model

The equilibrium state between the solid phase and the proteins are described with a modified Langmuir isotherm, Langmuir mobile phase modulator model (Langmuir MPM). The model is based on the assumption that the available sites are uniformly distributed. The fundamental competitive isotherm is described by equation 4.

$$\frac{\partial q_i}{\partial t} = k_{ads,i} \cdot c_i \cdot q_{\max,i} \cdot \left(1 - \sum_{j=1}^{n} \frac{q_j}{q_{\max,j}} \right) - k_{des,i} \cdot q_i \tag{4}$$

The mobile phase modulators describe changes in retention due to changes in salt concentrations. The mobile phase modulators are introduced into the competitive isotherm as described by equation 5-6. [2]

$$k_{ads,i} = k_{ads0,i} \cdot e^{\gamma_i \cdot S} \tag{5}$$

$$k_{des,i} = k_{des0,i} \cdot S^{\beta_i} \tag{6}$$

$$K_{eq} = \frac{k_{ads}}{k_{des}} \tag{7}$$

The electrostatic parameter, β, depends on the characteristic charge and charge distribution of the protein and the salt counter ion. The hydrophobicity parameter, γ, is dependent on the hydrophobic contact area upon bond formation and surface tension properties of the salt [2]. In an IEC process can the hydrophobicity parameter be neglected and set to zero, since the effect of hydrophobic interaction can be assumed to be negligible [3].

In multi-component systems the saturation capacity, q_{max}, of any individual component will affect the relative position and shape of all components [3]. Jacobson et al [4] suggest that the saturation capacity of the solute remains almost constant over the most useful range of variation of the mobile-phase composition. This assumption holds in a wide concentration range for molecules, whose conformation is not significantly altered by large changes in the composition of the solvent. It will, however, hold only in a limited range of the mobile-phase composition for large biomolecules [5].

In order to account for the saturation capacity changes is equation 8 introduced to regress the experimentally observed saturation capacity as a function of the elution strength modifier concentration. [6]

$$q_{\max,i} = \frac{\alpha}{1 + e^{\delta \cdot S + \zeta}} \tag{8}$$

where S is the elution strength modifier concentration and α, δ and ζ is experimentally fitted constants.

2.3 Simulation techniques

Simulation of the chromatographic process is performed with the BioSep-toolbox version 1.0 (Department of chemical engineering, Faculty of engineering, Lund University) in a Matlab environment.

The mass balance equations are integrated numerically using a finite difference method. The continuous (x, t) plane is replaced by the grid (Δx, Δt) and the and the differential equations replaced with the corresponding difference equations. The applied discretization method is of the fifth order with a backward difference for the first derivative and a center difference for the second derivative. A 60 grid point mesh is utilized to simulate the column. The differential equation set is solved by the built in ordinary differential equation solver ode15s in Matlab.

2.4 Model calibration

2.4.1 Primary parameter estimates

The saturation capacity of the column for each entity can be approximated from saturation experiments provided by the column manufacturer. Equation 9 provides a rough estimate of the saturation capacity (mol·m^{-3}) for a target entity, through scaling of a reference capacity with the molecular weight of the target entity. [3]

$$q_{\max,i} = \frac{cap_{ref} \cdot \left(Mw_{ref} / Mw_i \right) \cdot 1000}{\left(1 - \varepsilon_c \right) \cdot Mw_i} \tag{9}$$

where cap_{ref} is the reference capacity, Mw_{ref} the molecular weight of the reference entity, Mw_i the molecular weight of entity i and ε_c the column void. The reference entity should be in the same molecular weight range as the target entity in order to mimic the accessibility in the pores.

The flow dependent axial dispersion coefficient, D_{ax}, is calculated according to equation 10 under the assumption that the particle Peclet number, Pe, is constant. The Peclet number gives a quantitative measure of the rate of diffusion related to the rate of advection of a flow. For small Reynold numbers only little variation occurs in the Peclet number in packed beds, due to the insignificance of molecular diffusion effects in packed beds under laminar or low turbulence conditions [7].

$$Pe = \frac{\upsilon_{\text{int}} \cdot d_p}{D_{ax}} \tag{10}$$

where d_p is the particle diameter of the column packing and v_{int} the interstitial velocity.

Ishihara and Yamamoto [8] propose an approach to estimate the distribution coefficient as a function of the salt concentration, I, from the elution peak salt concentration, I_R. From this approach can the equilibrium association constant, K_{eq}, and the electrostatic parameter, β, be derived. The salt concentration at peak position I_R is determined as a function of normalized gradient slope, GH. The normalized gradient slope, GH, is defined by eqn 11 in linear gradient elution.

$$GH = \frac{I_F - I_0}{V_g} \cdot \frac{1 - \varepsilon_c}{\varepsilon_c} \cdot V_0 \tag{11}$$

where I_F is the final salt concentration, I_0 the initial salt concentration, V_g the gradient volume, V_0 is column void volume and ε_c the column void. The GH-I_R curves thus constructed do not depend upon flow velocity, column dimensions, sample loading at non-overloading conditions or the initial salt concentration provided that the sample is initially strongly bound to the matrix. The GH-I_R relationship is expressed by eqn 12.

$$GH = \frac{I_R^{(B+1)}}{A(B+1)} \tag{12}$$

Through regression of the logarithmic experimental data can A and B be determined. The expression is derived from the law of mass action and A is the equivalent of Henry's constant of absorption while B is the number of charges involved in protein adsorption and is an estimate of the electrostatic parameter, β. [8]

2.4.2 Calibration methods

The parameters that determine the behavior within the column is subjected parameter fitting against experimental data. In this paper is two different methodologies utilized: (i) Peak positioning and shape fitting and (ii) consolidation.

The peak position and shape fitting objective function aims at minimizing the mean squared residual through calibrating individual components. Four residuals are formed for each component and experiment in order to fit position, height and shape. The residuals are formed from normalized simulated and experimental data.

The consolidation is based on a sum of least square algorithm. The consolidation objective function aims at obtaining a convergence between experimental and simulated chromatogram. The objective function, equation 20, aims at minimizing the generalized residual. The objective function is intended to consolidate previous calibration steps and polish the solution.

2.5 Chromatographic optimization

Optimization of a chromatography step combines selection of equipment and experimental conditions to fulfill process requirements. The optimization typically aims at minimize an objective function, Q, through varying decision variables. The objective function is a function of the decision variables.

2.5.1 Objective functions

The most suitable objective function in industrial preparative chromatography applications would be production cost, but reasonable estimates of the cost figures are usually not available. Production rate is the objective function generally used in academic studies. The production rate, Pr, is the amount of feed purified at the required degree of purity per time unit, eqn 13.[9]

$$\mathrm{Pr}_i = \frac{V_s \cdot c_{0,i} \cdot Y_i}{\Delta t_c} \tag{13}$$

where V_s is the sample volume, c_0 the feedstock concentration, Y the recovery yield and Δt_c the cycle time. The cycle time, Δtc, is the time that separates to consecutive injections. The recovery yield is defined as the fraction of the loaded amount of target component which is recovered in the purified fraction as product, *see* eqn 14.

$$Y_i = \frac{\int_{t_1}^{t_2} c_i \, dt}{c_{o,i} \cdot t_{load}} \tag{14}$$

where $c_{0,i}$ is the feedstock concentration of component i, t_{load} is the loading time and c_i is the concentration of component i in the effluent.

2.5.2 Design parameters

Design parameters encompass parameters that cannot be changed during optimization. Typical examples are pH, feedstock concentration, buffer system and stationary phase matrix.

2.5.3 Decision variables

The number of decision variables in a chromatographic purification step is restricted, since to many decision variables gives to many degrees of freedom to obtain a solvable system [3]. The decision variables are changed in order to find maximum or minimum point of the target objective function.

Felinger and Guiochon [9] stated that many decision variables can be disregarded and that only two parameters affect the band profiles in non-linear chromatography: Column efficiency and loading factor.

Column efficiency in displacement chromatography with gradient elution is governed by the normalized gradient slope, GH (eqn 12). The loading factor, L_f, is the ratio between total amounts of species in the sample to the column saturation capacity, eqn 15.

$$L_f = \frac{V_s}{(1-\varepsilon_c)\cdot V_c} \cdot \sum_{i=1}^{n} \frac{c_i^0}{q_{\max,i}} \tag{15}$$

where V_s is the sample volume, V_c is the column volume, ε_c is the column void, $q_{max,i}$ the column capacity for component i and $c_{0,i}$ the feed concentration.

2.5.4 Constraints

Physical constraints, e.g. protein solubility, concentrations and activity, limit the possibilities to optimize protein chromatography. The physical constraints provide a framework for experimental design and an operating window where the model-based optimization can be performed. Industry requirements and process economics invoke quality constraints, e.g. purity, pool concentration, and buffer consumption that need to be considered in the optimization.

3 Experimental design

3.1 Materials

The experiments are performed with an ÄKTA Purifier 100 chromatography system (Amersham Biosciences). The utilized column is a 1 ml Resource 15Q (GE Healthcare, Uppsala).A dispersive mixture of bovine serum albumin (BSA) (Sigma-Aldrich, CAS: 9048-46-8) and Anti-FVII Mab (IgG), kindly provided by Novo Nordisk AS (Bagsværd, Denmark), is utilized in the experiments. A solution with a concentration of 4.11 mg·ml^{-1} BSA in 20 mM Tris-HCl, pH 8.5, was prepared.

IgG was obtained as a solution at an approximate concentration of 1,3 mg·ml^{-1} in a unknown buffer, pH 8. The IgG was desalted and recovered at a concentration of approximately 2.33 mg·ml^{-1} IgG in 20 mM Tris-HCl, pH 8.5. Buffer grade Tris-HCl (CAS:77-86-1) and NaCl (Code art.: 27800.360) was obtained from USB respectively VWR.

3.2 Methods

3.2.1 Determination of dead volumes

Determination of system dead was performed with low concentration ammonium solution with the column disconnected and mixing vessel was replaced by a T-junction.

3.2.2 Gradient experiments

Gradient experiments were performed to calibrate the simulated gradient. A linear gradient between 0 and 1 M NaCl was applied for gradient volumes of 0, 20, 40 and 60 CV. Gradient experiments are performed with disconnected column.

The correlation between salt concentration and conductivity was regressed from discrete measurement data for known molar fractions of elution buffer.

3.2.3 Determination of monomer content

The pure IgG and BSA standard solutions are separated according under conditions equivalent to optimization experiments. A 1 mL sample loop and gradient volumes of 20 and 40 CV were applied. UV-detection was performed at 280 nm. The relative quantity of monomer and impurity in each solution was determined through peak integration.

3.2.4 Model calibration experiments

The optimization is based on 2^2 stratified batch experiments varying loading factor and gradient slope. The sample solution is prepared at a concentration of 0.43 mg·ml^{-1} IgG and 1.28 mg·ml^{-1} BSA in 20 mM Tris-HCl buffer, pH 8,5. The sample is injected from a 1 ml sample loop. The variation in loading factor is obtained through diluting the sample 2:1. Applied gradients are of length 20 and 40 CV. The column was washed with 2 CV 20 mM Tris-HCl buffer. The flow rate is set to 4 ml·min^{-1} and UV detection is performed at 280 nm.

3.2.5 Optimization experiments

The obtained interim optimal loading volume and gradient length is applied to the calibration experiment method. The sample solution is injected from a 10 ml sample reservoir. Experiments are performed under same conditions as calibration experiments.

4 Simulation design

4.1 General methodology

The model-based optimization methodology suggested in this paper encompasses model calibration and optimization, based on a common simulation tool. The methodology is based on an iterative process, with continuous model refinement and addition of new experimental data. Initially is the salt concentration modeled and calibrated. Each consecutive optimization cycle is comprised of three steps:

i. Fitting and refining of parameter set.
ii. Optimization of process conditions.
iii. Addition of new experimental data.

The obtained interim optimal experimental conditions are applied to the experimental method. Obtained interim optima are added to the experimental reference data. The cycle is reiterated until the adequate results are obtained.

The key parameters that determines the behavior of the entities within the simulated column is identified. Typically these are the shape and peak position determining parameters. The key parameters are targets for the parameter estimation, due to their impact on obtained results. The identified key parameters are K_{eq}, k_{des}, β and the capacity modulators α, δ and ς..

In order to reduce the number of components and parameters to be calibrated is only the major components in the relevant elution interval evaluated. The tailing IgG impurities are merged. This result in BSA yielding two peaks, BSA monomer and BSA dimer, and IgG yields two peaks; the IgG monomer and IgG impurities.

4.2 Model calibration

Firstly a primary parameter set is estimated to roughly mirror the experimental behavior. The initial parameter set is estimated according to above mentioned methodologies and gathered from literature. The estimate of the capacity factor serves as an initial proxy for the capacity modulator α. The electrostatic parameter and K_{eq} is estimated by the approach suggested by Yamamoto and Ishihara [8]. The key parameters are manually tuned to place peak positions within the interval defined by peak base widths and to obtain simulated peak heights that approaches experimental values.

The model refinement procedure aims at obtaining convergence between simulated and experimental data. The utilized estimation tools are expressed above. The parameter estimation tool is the calibration divided into three parts. The following methodology is applied:

i. *Fitting of peak position and shape for individual distinguishable peaks*. The isotherms are calibrated separately through fitting of parameter set for individual distinguishable components.
ii. *Unified fitting of peak position and shape for distinguishable peaks*. The isotherms are calibrated through simultaneous fitting of parameter set for all distinguishable components.
iii. *Consolidation of parameter estimation*. In order to polish the solution and consolidate the estimation is the simulated chromatogram fitted against the experimental chromatogram.
iv. *Review of obtained parameter values*. Obtained parameter values are evaluated. Acceptable results initiate the optimization and non-acceptable results initiate a new calibration cycle.

The shape and position objective function is minimized by a Nelder-Mead simplex method executed by the

Matlab function fminsearchbnd in order to allow bounded variables and thus avoid unreasonable parameter values. The consolidation objective function is minimized by least square means and executed by the built in Matlab function lsqcurvefit.

Undistinguishable peaks in the optimization experiments are fitted against performed standard solution experiments. Due to the lack of specific experimental data is the initial parameter set not refined.

4.3 Optimization

The optimization targets purification of the BSA monomer regarding productivity. Sample volume and gradient volume is set as decision variables for the optimization.

The cycle time is defined as the time between consecutive injections, i.e. the sum of time consumption for load, wash, elution, regeneration and equilibration. The regeneration time is assumed to be independent of sample concentration and gradient concentration and is hence constant. The time consumption of regeneration and equilibration is set to 15 ml.

The optimization is performed utilizing Newton's method with the built in Matlab function fmincon.

The optimization is subjected to a 99 wt% purity constraint regarding BSA monomer relative to the total content of BSA and IgG monomer.

5 Results and discussion

5.1 Simulation prerequisites

The IgG standard solution was found to have a content of 83% monomer, while the BSA solution was found to have a monomer content of 77.5%. The injection pre-column dead volume was determined to be 0.14 ml and the buffer pre-column dead volume was determined to 0.66 ml. The dead volume between the UV-vis flow cell and the conductivity flow cell was determined to be approximately 0.2 ml.

The simulated gradients show compliance with the experimental data. The compliance is significantly lower for steep gradient slopes than for moderate gradient slopes.

Performed experiments are subjected to a number of uncertainties linked to protein concentrations. The sample preparation is subjected to variances in pipettes and scales as well as inaccuracy in concentration determinations. Even small deviations have significant impact due to the magnification by the absorption factors.

5.2 Model

It has been shown in prior work by El Fallah and Guiochon that prediction of column behavior requires incorporation of mobile phase and stationary phase non-idealities. The introduction of the mobile phase modulator and the saturation capacity modulator are a response to this. The need for accounting for non-idealities holds true especially for steep gradients and high loading factors, where significant discrepancies has been observed.[5]

One drawback of the constructed adsorption model is that a uniform behavior is assumed for each component. In reality all components have multiple sites with different ionization properties. This will cause a deviation from ideality and cause peak tailing. Binding occurs in both weak and strong sites as well as in combination through avidity. The model is incapable of accurately predicting this behavior. This would probably be described better by e.g. a bilangmuir isotherm.

Modeling all non-idealities and mass transport within the column is not desirable, since it would yield too many parameters to determine. The constructed model is subjected to a trade off between reflecting physical behavior and limiting computational time and number of calibrated parameters.

5.3 Model calibration

The model is calibrated through three consecutive cycles to yield the conclusive parameter set, *see* Table 1. The obtained parameter set shows a good fit to the optimization experiments, see Figure 1.

Table 1. Conclusive parameter set for protein components.

	IgG anti-FVII		BSA	
Parameter	Monomer	Impurity	Monomer	Dimer
K_{eq}	0.442	0.3	0.429	10.78
β	5.78	7	6.72	7.21
k_{des}	19288	2086	14179	3568
a	$6.47 \cdot 10^{-4}$	$2.77 \cdot 10^{-2}$	$9.12 \cdot 10^{-4}$	$2.91 \cdot 10^{-4}$
ς	1.29	10.0	4.09	7.39
δ	0.674	3.0	0.964	1.54

The estimation approach suggested by Ishihara and Yamamoto [8] is not entirely suitable for the applied adsorption model. The approach yields an accurate prediction of peak position and proper spacing between elution peaks, but the peak shape is non-satisfactory. Obtained high electrostatic constants and low equilibrium constants result in unreasonable peak

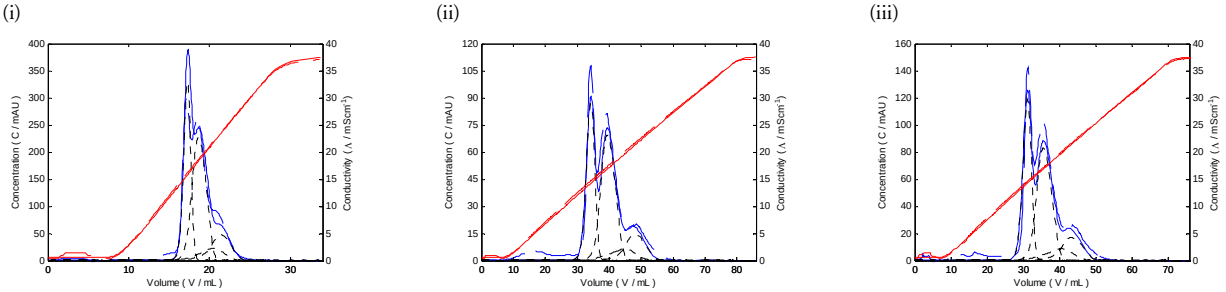

Figure 1. Final model calibration for optimization experiments: (i) Gradient volume 20.7 CV and loading volume 3.74 mL, (ii) gradient volume 74.5 CV and loading volume 2.95 mL and (iii) gradient volume 65.3 CV and loading volume 3.25.

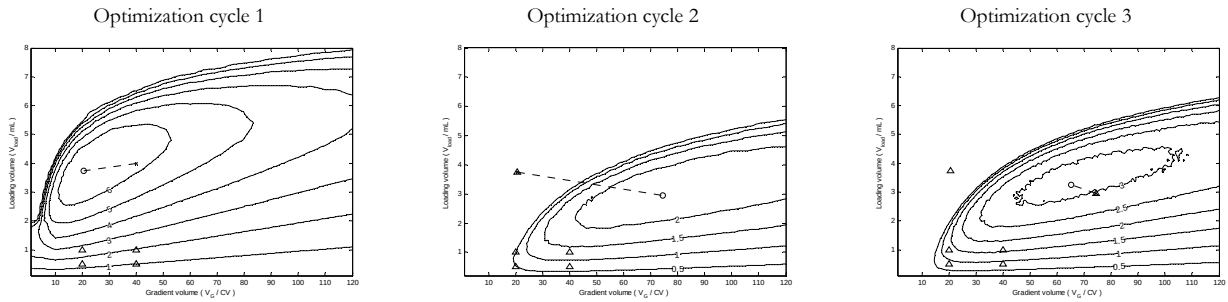

Figure 2. Propagation of optimal point of operations through the optimization cycles plotted on the productivity contours, where (x) is the initial guess value, (o) is the obtained optimal operation point and (Δ) represents model calibration points.

compression. An extensive leading edge is obtained and the error between experimental and simulated data from lack of tailing peaks propagates along the chromatogram. The introduction of the saturation capacity modulators alleviates the issue of extensive leading edges and provides a better fit to overloaded conditions and short gradients. The saturation capacity modulators allows lower values for the electrostatic parameter through providing spacing between elution peaks at different gradients and shaping the elution peaks. The results are improved but the issue of inadequate tailing remains. Manual tuning attempts also show that high values for the saturation capacity modulator denominator parameters yield instability due to a high degree of component interaction in the model.

One of the main issues in the calibration methodology is the inadequacy to search for an objective function minimum globally. Utilized methods likely linger on local minima, which prevent large scale improvements in calibration without manual tuning. Another inadequacy of the calibration methodology is the inability to resolve the juxtaposing character of the equilibrium constant and the electrostatic parameter. Utilized simplex method and least square method are unable to tune these parameters in any greater extent. As a direct consequence is manual tuning needed to fit the elution peak position. A requirement for successful implementation is a calibration methodology capable of searching for the solution on a large scale.

5.4 Optimization

The productivity of the process appears to be limited by the BSA dimer zone spreading, due to the during calibration progressingly growing leading edge. It is expected that the significantly larger IgG monomer content (wt%) in combination with the anticipated tailing that the IgG monomer is the limiting factor. The effects of the calibration inadequacy in forming tailing peaks spill over to the optimization results.

The productivity surface is abrasive in the domain where the optimum is expected to be found. This results in that the optimization lingers on local maxima within the domain, due miniscule step sizes. The productivity surface shows that there is not a stable optimal point, but rather an appropriate range of loading and gradient volumes that provides adequate productivity. Special considerations should be taken concerning choice of loading volume. The steep slope of the productivity surface at overloading incurs a risk of not fulfilling the purity demand in production due to deviations in production conditions or fallacy of the model-based optimization.

The relative position of The IgG impurity relative to the BSA monomer makes IEC an unsuitable method for separation. The applied process is rather a capture step targeting BSA monomer and further unit operations are a necessity for elimination of the IgG impurity.

Table 2. Optimization results.

		Cycle		
		I	II	III
Loading volume	mL	3.74	2.95	3.25
Gradient volume	CV	20.68	74.47	65.32
Productivity	$mg \cdot h^{-1}$	6,94	2.41	3.21
Recovery yield	%	68.55	61.85	68.41
Purity	wt%	99.004	99.002	99.003
IgG monomer	wt%	0.142	0.100	0.0655
BSA dimer	wt%	0.854	0.898	0.9312
Calibration MSE	-	0.164	0.147	0.234

6 Conclusions

The applied methodology is able to give a good fit between simulated and experimental data. The degree of agreement between experimental and calculated band profiles in gradient elution chromatography depends on the steepness of the gradient and on the loading factor. A good agreement is obtained for experiments well below overloaded conditions and for moderate gradient slopes. In order to be able to limit the amount of preparatory experiments is a potent calibration methodology capable of finding the global minima a central prerequisite. The calibrated parameter set and applied chromatographic model fails to account for the peak tailing, which results in a global error at the end of the clustered elution peaks. The introduction of saturation capacity modulators alleviates the extensive leading edges in the Langmuir MPM model with high electrostatic parameters. The tailing is central for a good model calibration and for accurate prediction of the optimal operation point.

7 References

[1] G. Guiochon, S. Golshan-Shirazi, A.M. Katti, Fundamentals of Preparative and Nonlinear Chromatography, AcademicPress, Boston, 1994.

[2] W.R. Melander, Z. El Rassi, C. Horváth, J. chromatography, 469 (1989), 3.

[3] N. Jakobsson, A model-based approach to robustness analysis and optimisation of chromatography processes. Chemical Engineering, Lund University, 2006.
[4] J. Jacobson, J. Frenz, C. Horvath, J. Chromatogr. 316 (1984) , 53..

[5] M.Z. El Fallah, G. Guiochon, Anal. Chem. 63 (1991), 2244.
[6] L. Melter, A. Butté, M. J. Morbidelli, Chromatogr. A, 1200 (2008), 156.

[7] J.M. Coulson, J.F. Richardson, J.R. Brackhurst, J.H. Harker, Chemical engineering, volume 2, Pergamon, Oxford, 1991.
[8] T. Ishihara, S. Yamamoto, J. Chromatogr. A, 1069 (2005), 99.
[9] A. Felinger, G. Guiochon, J. Chromatogr. A, 796 (1998), 59.
[10] A. Felinger, G. Guiochon, J. Chromatogr. A, 609 (1992), 35.